Processing of eukaryotic Okazaki fragments by redundant nucleases can be uncoupled from ongoing DNA replication *in vivo*

Malik Kahli[†], Joseph S. Osmundson[†], Rani Yeung and Duncan J. Smith[*]

Department of Biology, New York University, New York, NY 10003, USA

ABSTRACT

Prior to ligation, each Okazaki fragment synthesized on the lagging strand in eukaryotes must be nucleolytically processed. Nuclease cleavage takes place in the context of 5′ flap structures generated via strand-displacement synthesis by DNA polymerase delta. At least three DNA nucleases: Rad27 (Fen1), Dna2 and Exo1, have been implicated in processing Okazaki fragment flaps. However, neither the contributions of individual nucleases to lagging-strand synthesis nor the structure of the DNA intermediates formed in their absence have been fully defined *in vivo*. By conditionally depleting lagging-strand nucleases and directly analyzing Okazaki fragments synthesized *in vivo* in *Saccharomyces cerevisiae*, we conduct a systematic evaluation of the impact of Rad27, Dna2 and Exo1 on lagging-strand synthesis. We find that Rad27 processes the majority of lagging-strand flaps, with a significant additional contribution from Exo1 but not from Dna2. When nuclease cleavage is impaired, we observe a reduction in strand-displacement synthesis as opposed to the widespread generation of long Okazaki fragment 5′ flaps, as predicted by some models. Further, using cell cycle-restricted constructs, we demonstrate that both the nucleolytic processing and the ligation of Okazaki fragments can be uncoupled from DNA replication and delayed until after synthesis of the majority of the genome is complete.

INTRODUCTION

The synthesis of each Okazaki fragment requires several distinct enzymatic activities (1). The primase component of the Pol α-primase complex synthesizes a short RNA primer, which is further extended by the error-prone DNA polymerase α (Pol α) (2,3). The high-fidelity, PCNA-associated polymerase δ (Pol δ) is subsequently loaded onto the 3′ terminus of the initiating fragment in a reaction catalyzed by the RFC clamp loader (4). Pol δ synthesizes DNA to the 5′ end of the preceding fragment and continues beyond this point (5), generating a 5′ flap structure. The displaced 5′ flap serves as a substrate for nucleases (6), which cleave to generate a nick between Okazaki fragment termini. Iterative rounds of extension, followed by flap cleavage or nick regeneration by the 3′-5′ exonuclease activity of Pol δ (5), maintain a ligatable nick that persists until it is sealed by DNA ligase I, encoded by the *CDC9* gene in *Saccharomyces cerevisiae* (7). Nuclease cleavage during Okazaki fragment biogenesis represents an extremely abundant DNA transaction – one that must occur tens of thousands of times during each S-phase in *S. cerevisiae* and millions of times per human cell division.

The nucleases Rad27 and Dna2 have been proposed to cleave the majority of flaps during Okazaki fragment maturation. Genetic and biochemical work has given rise to a 'two-nuclease' model (1,8). According to this model, (9) iterative extension by Pol δ is followed by immediate cleavage of short DNA flaps by Rad27. If Pol δ extension outpaces Rad27 cleavage, Dna2 is required to process the resulting long flap. Rad27 and Dna2 show distinct substrate requirements *in vitro*. Rad27 readily cleaves short flaps; longer flaps are competent to bind RPA and thereby become refractory to Rad27 cleavage (10). Long, RPA-coated flaps are optimal substrates for Dna2 *in vitro*. Dna2 cleaves to leave a short flap such that RPA dissociates and Rad27 can cleave (11,12). However, recent reports indicate that Dna2 activity is sufficient to process 5′ flaps into ligatable nicks *in vitro* (13). Genetic data suggest additional redundancy in lagging-strand processing, and point to the likely involvement of Exo1 as a third Okazaki nuclease. *In vivo* in *S. cerevisiae*, neither *RAD27* nor *DNA2* is strictly essential for replication or viability because the lethality of *dna2* null mutants can be suppressed by deletion of *RAD9* (14,15). Furthermore, the temperature-sensitive phenotypes of both *rad27* and *dna2-1* can be suppressed by overexpression of *EXO1* (16–18). Despite the apparent contribution of at least

three deoxyribonucleases to lagging-strand processing, the normal contribution of each nuclease has not been clearly defined *in vivo*.

It is currently unclear whether impaired lagging-strand processing *in vivo* would predominantly give rise to reduced nick translation by Pol δ and associated nucleases, or to residual Okazaki fragment 5′ flaps resulting from ongoing strand-displacement synthesis by Pol δ without coupled nuclease cleavage. *In vitro* data suggests that strand-displacement synthesis by Pol δ should be dramatically reduced by a failure to cleave Okazaki fragment termini; instead, idling by Pol δ should maintain genomic nicks after limited strand displacement (5,19). However, electron microscopy analysis of DNA purified from *Schizosaccharomyces pombe* with lagging-strand processing defects detected the accumulation of long flap structures at ∼1-2% of Okazaki fragment termini (20): because shorter flaps would be undetectable by electron microscopy, the extent of residual flap formation in lagging-strand processing mutants is unclear. Furthermore, the ability of the replisome to bypass damage *in vivo* (21,22) and *in vitro* (23) suggests that DNA repair can occur after bulk DNA synthesis. This model is supported by additional *in vivo* evidence – for example the ability of *S. cerevisiae* to defer post-replication repair to G2/M (24). Lagging-strand synthesis must inevitably occur at the same time as the leading strand, but the extent to which Okazaki fragment processing must be coupled to ongoing replication has not been determined.

Here, we conduct a systematic analysis of lagging-strand processing in *S. cerevisiae* while depleting the lagging-strand nucleases Rad27, Dna2 and Exo1 in all possible combinations. In all cases, we co-deplete DNA ligase and therefore analyze mature lagging-strand products, which we refer to as Okazaki fragments. Our data are consistent with a model whereby the extent of strand-displacement by Pol δ is severely reduced in the absence of nuclease cleavage. Rad27 cleaves most lagging-strand flaps, Exo1 serves as a redundant processing factor when Rad27 is absent, and the contribution of Dna2 to lagging-strand processing in the uniquely mappable regions of the *S. cerevisiae* genome is limited. Further, we show that cells remain viable when Okazaki fragment ligation is deferred until after bulk DNA synthesis in each cell cycle; nucleolytic processing of the lagging strand can be similarly deferred, but only if the accumulation of single-stranded DNA is mitigated during S-phase.

MATERIALS AND METHODS

Yeast strains, cell growth and spot tests

Yeast strains were all W303 RAD5+. The wild type strain genotype is *matA, tor1-1::HIS3, fpr1::NatMX4, RPL13A-2xFKBP12::TRP1, CDC9-FRB::KanMX6*. Additional FRB tagging, gene deletions, Clb2 promoter insertion and myc tagging were performed by PCR-mediated replacement, and introduced into the parent strain by crossing. At least two independent replicates of each strain were selected after tetrad dissection.

For *GAL1-SSB* strains, the pRS405 integrating vector containing a codon-optimized open reading frame encoding *E. coli* SSB under the control of the *GAL1* promoter was integrated at the *LEU2* locus. Stains were grown at 30°C in YPD unless otherwise specified. Rapamycin was added to a final concentration of 1 g/ml in liquid media or 2 g/ml in solid media. For spot tests, cells were washed and diluted to an OD of 1. Cells were plated at a 1:10 dilution series and grown overnight at 30 or 37°C as specified.

Cell-cycle synchronization and western blotting

200ml of exponential phase cell cultures at OD 0.3–0.4 was synchronized in G1 using 5g/ml alpha factor. Cells were released into S-phase and harvested at different time points. Growth was immediately stopped by addition of ice cold water and cells were centrifuged at 4°C. Cells were resuspended for 5 min in 2 M lithium acetate at 4°C, pelleted, resuspended for 5 min in 400 mM sodium acetate at 4°C, pelleted again and finally resuspended in 1× Laemmli buffer plus 5% beta-mercaptoethanol. After 5 min of boiling at 100°C, the lysates were centrifuged for 5 min at top speed and transferred to new tubes prior to loading on a 10% SDS-PAGE gel. After migration at 100 V, samples were transferred to a PVDF membrane, blocked with 5% milk in TBS–0.1% Tween and probed with a C-Myc antibody (Genscript A00173-100). Loading controls were done by Coomassie staining of gels loaded with identical amounts of sample and run alongside gels for Western blots.

Fluorescence-activated cell sorter (FACS) analysis

150 μl of cells were harvested during the S-phase release at different timepoints and 350μl of 100% ethanol was added to fix the cells overnight at 4°C. Cells were pelleted, resuspended in 50 mM sodium citrate plus Rnase A and incubated at 50°C for 1 h. After addition of proteinase K and another hour of incubation, cells were labeled with SYTOX green and stored at 4°C before analysis using a Becton Dickinson Accuri.

Okazaki fragment analysis

Okazaki fragments were purified and end-labeled essentially as described (25). Briefly, DNA concentration was normalized by Qubit. 650 ng of DNA per lane was treated with Klenow (exo-) (NEB) and α-[32]P dCTP for 30 min at 37°C in NEBuffer 2. Unlabeled nucleotides were removed using Illustra G50 columns (GE Healthcare) and samples were separated for 5 h at 77 V in 1.3% alkaline agarose gels. DNA was transferred to a Nylon membrane overnight and visualized using a phosphorimager.

For *in vitro* ligation experiments, samples were incubated in 1× DNA ligase buffer (NEB). 2 μl of T4 DNA ligase (NEB) was added and samples were incubated for 90 min at room temperature before phenol extraction and end-labeling.

Okazaki fragment purification and sequencing was carried out as previously described (25). Paired-end sequencing (2 × 75 bp) was carried out on an Illumina Next-seq 500 platform.

RESULTS

Systematic depletion of Okazaki nucleases and analysis of lagging-strand products

DNA2 is an essential gene in checkpoint-proficient *S. cerevisiae* (14), and *rad27Δ* mutants have several undesirable phenotypes including slow growth and elevated mutation rate (26). In addition, genetic interactions between lagging-strand nucleases render double- and triple-mutant strains inviable or extremely sick (17). Therefore, we used the anchor away conditional nuclear depletion strategy to analyze lagging-strand processing in the absence of Rad27 and Dna2. Anchor away depletion is mediated by dimerization of FRB-tagged nuclear proteins with FKBP-tagged ribosomal subunits, and rapidly depletes proteins from the nucleus (27). We constructed a panel of *S. cerevisiae* strains carrying all possible combinations of *exo1Δ*, *RAD27-FRB* and *DNA2-FRB*, in combination with an FRB-tagged allele of *CDC9* for simultaneous co-depletion of DNA ligase. All proteins were tagged at the C-terminus. Two biological replicates of each strain were obtained via sporulation of a diploid strain heterozygous at the *EXO1*, *DNA2* and *RAD27* loci and homozygous at the *CDC9* locus. Conditional nuclear depletion of Rad27 or Dna2 recapitulated the reported phenotype of the null mutants (Figure 1A). *DNA2-FRB* strains were inviable upon rapamycin treatment, and *RAD27-FRB* strains were inviable at 37°C in the presence of rapamycin. Double (Figure 1A) and triple (not shown) nuclease mutants were inviable upon rapamycin treatment as expected.

Fully processed Okazaki fragments in *S. cerevisiae* are normally sized according to the nucleosome repeat length due to interactions between Pol δ and nascent chromatin behind the replication fork, and are poised for ligation after purification (25). We analyzed the size distribution of fragments from asynchronous cultures of strains depleted for DNA ligase and either one, two or all three nucleases, and further analyzed the extent to which these fragments were competent for ligation after purification of genomic DNA (Figure 1B, (25)).

Lagging-strand synthesis in the absence of one, two or three of the Okazaki nucleases did not lead to a gross change in fragment length (Figure 1B). However, depletion of Rad27 from the nucleus consistently led to a loss of the nucleosome patterning observed in Rad27-proficient strains. In all strains proficient for Rad27, treatment with T4 DNA ligase after DNA purification resulted in a significant loss of Okazaki fragment end-labeling regardless of the presence or absence of other nucleases (Figure 1B, quantified in Figure 1C). We note that the loss of ~45% of end-labeling signal upon ligase treatment is likely to provide a low estimate of the fraction of lagging-strand products poised for ligation. Therefore, we conclude that the majority of Okazaki fragments in strains with functional Rad27 are poised for ligation. By contrast to Rad27 proficient strains, depletion of Rad27 invariably led to Okazaki fragments that could not be ligated after purification (Figure 1B and C). Thus, lagging-strand products in the absence of Rad27 do not have 5′ and 3′ ends precisely juxtaposed for ligation, sug-

gesting that structures with flaps or gaps are prevalent when Rad27 is absent.

Okazaki fragment processing of nucleosomal DNA *in vivo*

In wild-type *S. cerevisiae*, Okazaki fragment 5′ and 3′ termini are normally enriched at nucleosome dyads; a shift in this distribution towards the replication-fork-proximal edge of the nucleosome indicates reduced nick translation by Pol δ and associated nucleases (25,28). It is further possible to distinguish reduced nick translation from ongoing strand-displacement synthesis in the absence of nuclease cleavage by comparing the locations of the 5′ and 3′ ends of mature Okazaki fragments: reduced nick translation would leave juxtaposed termini, whereas extensive strand displacement would generate 5′ and 3′ ends that peak at different points in the nucleosome. To directly investigate the extent of strand-displacement synthesis by Pol δ and nucleolytic lagging-strand processing in nucleosomal DNA, we purified and sequenced Okazaki fragments from asynchronous cultures (25) after co-depletion of Cdc9 and all combinations of nucleases for 1h. Distributions of Okazaki fragment termini around nucleosome dyads are shown in Figure 2. All data were highly reproducible across two biological replicates. Data from the second replicate corresponding to Figures 2 and 3 are shown in Supplementary Figure S1. For each sample, data were normalized to the maximum signal in the range to facilitate comparison between samples.

Consistent with a global reduction in strand-displacement synthesis by Pol δ when processing nucleases are depleted, fragment 5′ (Figure 2A) and 3′ (Figure 2B) termini showed similar distributions within each sample. If strand displacement were occurring in the absence of nuclease cleavage, 3′ ends would show a wild-type distribution with respect to nucleosomes, while 5′ ends would shift to more upstream locations. Depletion of Rad27 led to a pronounced shift in both 5′ and 3′ termini towards the replication-fork proximal edge of the nucleosome. Therefore, when Rad27 is absent, nick translation is substantially impaired even though most Okazaki termini are apparently not precisely juxtaposed (Figure 1B and C). Deletion of *EXO1* produced a lesser shift in the same direction, while depletion of Dna2 did not significantly impact Okazaki fragment terminus location. Additional depletion of Dna2 did not dramatically alter the location of termini in *RAD27-FRB* or *exo1Δ* strains. However, cells lacking both Exo1 and Rad27 activity showed an additional shift compared to each single mutant, consistent with redundancy between the two nucleases. Okazaki fragment distributions in the *RAD27-FRB DNA2-FRB exo1Δ* strain were similar to those in *RAD27-FRB exo1* (Figure 2A and B). Taken together, this suggests that depletion of Dna2 to levels that do not support viability does not have a significant impact on nucleosomal Okazaki fragment processing throughout most of the genome, even when one or both of the other Okazaki nucleases are absent. The distribution of Okazaki fragment termini supports a model whereby Rad27 processes the majority of 5′ flaps, with a minor contribution from Exo1 and an extremely limited role for Dna2.
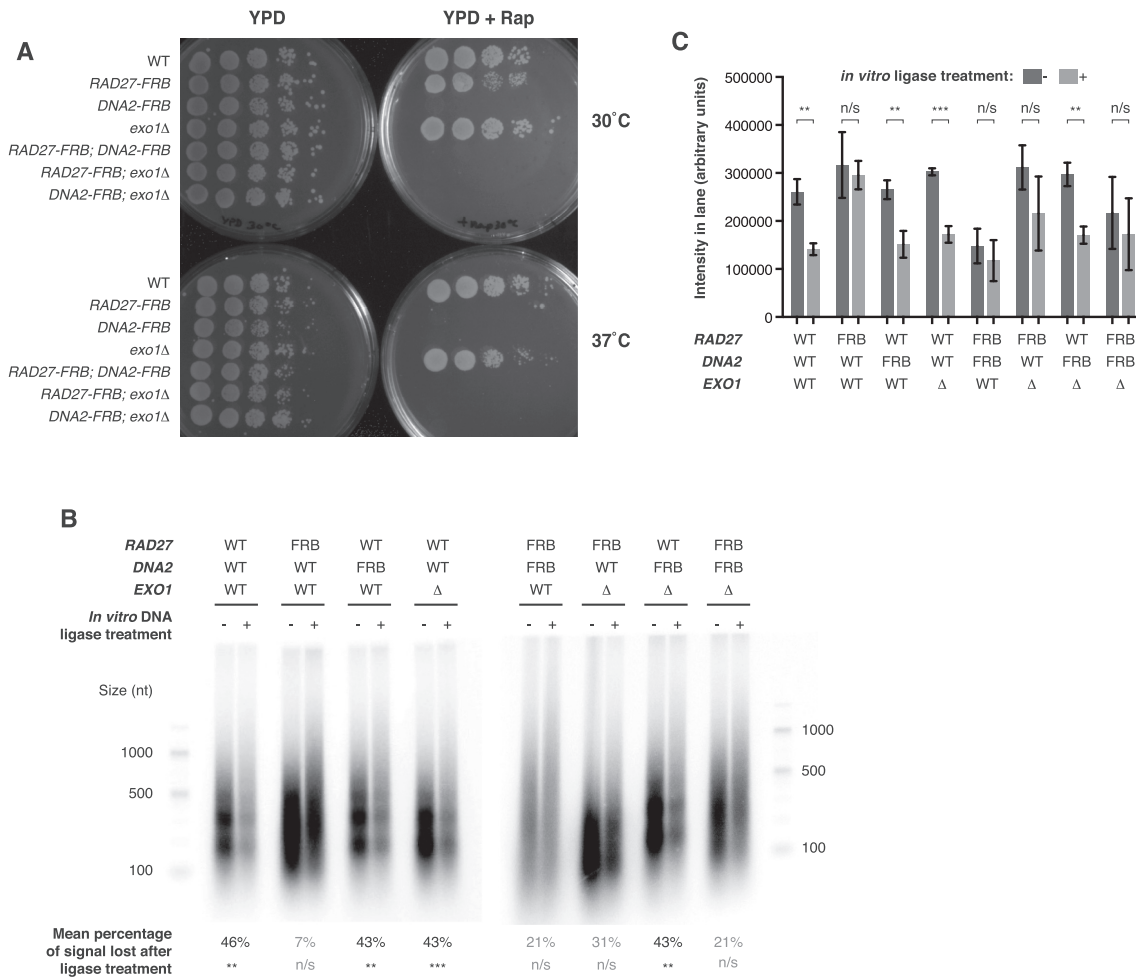
Figure 1. Enrichment of ligation-competent Okazaki fragments from strains lacking both lagging-strand nucleases and DNA ligase I. (**A**) Spot tests of indicated strains on YPD $\pm$ 2 μg/ml rapamycin at 30 or 37°C, as indicated, for single and double mutant strains analyzed in this study. Addition of rapamycin depletes FRB-tagged proteins from the nucleus. (**B**) End-labeled Okazaki fragments obtained after 1 h rapamycin treatment to deplete DNA ligase I and FRB-tagged nucleases. Where indicated, DNA was treated with T4 DNA ligase after purification but before labeling to assess the proportion of Okazaki fragments poised for ligation. WT denotes an otherwise wild-type *CDC9-FRB* strain. The percentage of signal lost upon ligase treatment, calculated from three replicates and shown graphically in (C), is indicated under each pair of lanes. In both (**B**) and (**C**), *P* values for differences between paired samples with and without ligase were calculated by *t*-test. *** denotes $P < 0.001$, ** denotes $P < 0.01$, n/s denotes $P > 0.05$. (**C**) Quantification of Okazaki fragment end-labeling signal from (B). The cumulative signal from the region corresponding to sizes <1000 nt was calculated for three replicate experiments, of which (B) is a representative example. Mean $\pm$ SD is plotted and *P* values are as in (B).

Okazaki fragment processing of non-nucleosomal DNA *in vivo*

In nucleosome-free regions, Okazaki fragment termini are normally enriched immediately upstream of binding sites for the transcription factors Abf1, Reb1 and Rap1. These transcription factors re-associate quickly following DNA replication, and appear to represent 'hard' barriers to Pol δ in contrast to the 'soft' barrier activity of nucleosomes (25). We analyzed the distribution of Okazaki fragment termini around these transcription factor binding sites, as a means to investigate strand-displacement and processing on non-nucleosomal templates (Figure 3). Data were normalized to the median signal within the range in order to assess the propensity of Pol δ to terminate specifically at transcription-factor binding sites as opposed to nearby sequences.

In both wild-type and single nuclease depletions, we observed a prominent peak of Okazaki fragment 5′ and 3′ termini immediately upstream of a meta-binding site for Abf1/Reb1/Rap1 (Figure 3 A&B). However, the *RAD27-FRB exo1Δ* strain showed significantly reduced termination on the replication-fork proximal edge of the transcription-factor binding sites relative to the wild-type strain. The *RAD27-FRB DNA2-FRB*; *exo1Δ* strain generated slightly fewer fragments terminating at transcription-factor binding sites than the *RAD27-FRB exo1Δ* double mutant, suggesting that the decreased strand-displacement and nick translation on non-nucleosomal DNA in the absence of both Rad27 and Exo1 can be further reduced by removal of Dna2. These data are consistent with a globally similar distribution of nuclease activity on non-nucleosomal DNA to that observed within nucleosomes—i.e. major redundant roles for Rad27 and Exo1 and a limited role for Dna2. However, the distribution of Okazaki fragment termini around TF binding sites in both *RAD27-FRB* and *exo1Δ* strains
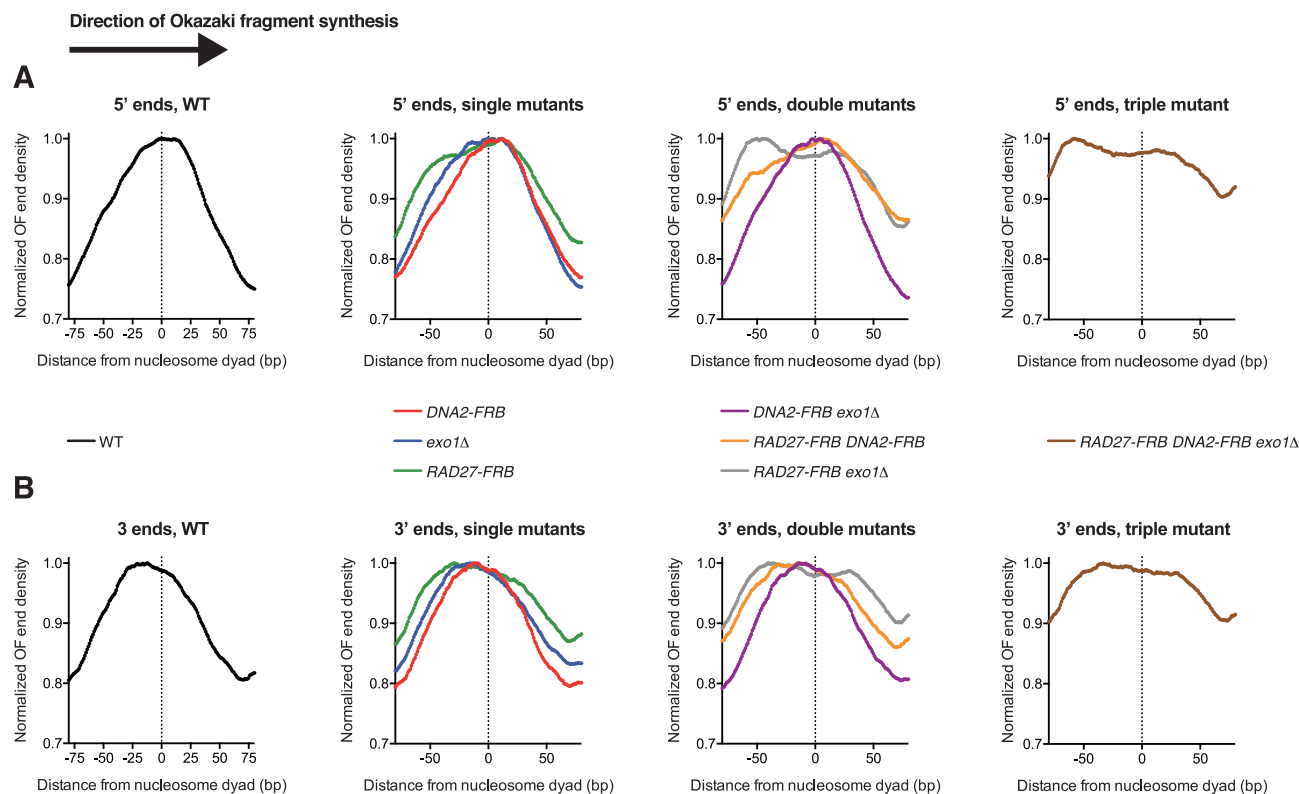
Figure 2. Contributions of individual nucleases to Okazaki fragment processing in the context of nucleosomal DNA. (**A**) Distribution of Okazaki fragment 5′ termini around consensus dyad locations of the top 50% most highly occupied nucleosomes in the *S. cerevisiae* genome (38). WT, single mutants, double mutants and the triple mutant are displayed in separate graphs for clarity. Data are presented such that Okazaki fragment synthesis proceeds from left to right. Data are normalized to the maximum signal in the range, and smoothed to 5 bp. (**B**) Distribution of Okazaki fragment 3′ termini around nucleosome dyads, as in (A).

closely resembles that of a wild-type strain (Figure 3A and B). Therefore, our data suggest more extensive redundancy of Rad27 and Exo1 outside nucleosomes than on nucleosomal templates.

Uncoupling of Okazaki fragment processing from DNA synthesis

To investigate the extent to which the processing and ligation of the lagging strand can be uncoupled from its synthesis *in vivo*, we constructed strains in which expression of *RAD27*, *DNA2*, *EXO1* or *CDC9* was driven by the *CLB2* promoter, and the protein fused to the N-terminal degron of the Clb2 protein. Expression of such *CLB2*-tagged constructs is limited to very late S- and G2 phase (29). Myc-tagged versions of Clb2-Cdc9, Clb2-Rad27, Clb2-Exo1 and Clb2-Dna2 were detectable by western blot: all proteins displayed the anticipated cell cycle expression profile, with expression limited to late S/G2 (Supplementary Figure S2A–F). The lower band in the Cdc9 blot represents the mitochondrial isoform of Cdc9 (30), which does not cycle in a cell cycle-dependent manner.

Sporulation of a heterozygous diploid *CLB2-CDC9/CDC9* strain produced four viable spores per tetrad, indicating that expression of DNA ligase I exclusively at the end of S-phase and in G2 is sufficient to support viability (Figure 4A). Consistent with delayed ligation of Okazaki fragments when *CDC9* expression is restricted, the *CLB2-CDC9* strain transiently accumulated Okazaki fragments following release from G1 arrest which disappeared when ligation was enabled by *CLB2-CDC9* expression in late S/G2 (Figure 4B). Sporulation of a *CLB2-RAD27/RAD27 CLB2-EXO1/EXO1* strain also generated four viable spores per tetrad, although *CLB2-RAD27 CLB2-EXO1* double mutant haploids grew slowly (Figure 4C). *CLB2-RAD27* cells phenocopied the temperature-sensitivity and slow growth of *rad27* cells, suggesting that these phenotypes arise due to a lack of Rad27 during S-phase (Supplementary Figure S2G). The observation that Rad27 and Exo1 together process the majority of Okazaki fragments in *S. cereivisiae* (Figures 2 and 3), but can maintain viability when expressed only after the bulk of replication has been completed, suggests that Okazaki fragment processing need not occur concurrently with replication.

Sporulation of a *CLB2-RAD27/RAD27 CLB2-DNA2/DNA2* strain produced a mixture of viable and inviable spores (Figure 4D). Colonies formed from *CLB2-DNA2* spores have an essentially wild-type growth phenotype (Figure 4D). Thus, the essential contribution of Dna2 to viability can apparently be executed after the majority of the genome has been synthesized. In contrast to *CLB2-RAD27 CLB2-EXO1* double mutants, *CLB2-RAD27 CLB2-DNA2* haploids are inviable (Figure 4D).
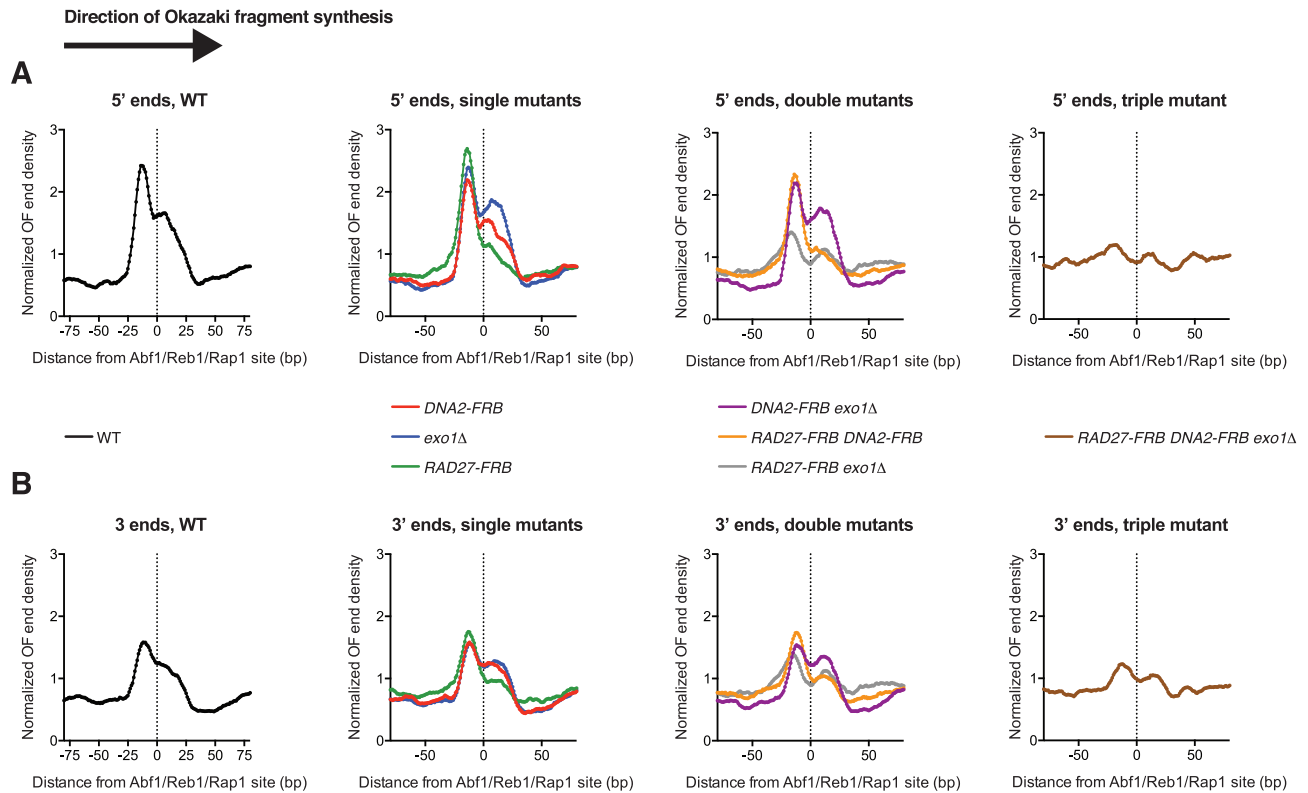
Figure 3. Contributions of individual nucleases to Okazaki fragment processing in the context of non-nucleosomal DNA. (**A**) Distribution of Okazaki fragment 5′ termini around binding sites for Abf1, Reb1 and Rap1 (25,39). As in Figure 2, WT, single mutants, double mutants and the triple mutant are displayed in separate graphs for clarity. Data are presented such that Okazaki fragment synthesis proceeds from left to right. Data are normalized to the median signal in the range, and smoothed to 5 bp. (**B**) Distribution of Okazaki fragment 3′ termini around binding sites for Abf1, Reb1 and Rap1, as in (A).

Therefore, although Exo1 apparently contributes to the overall processing of Okazaki fragments to a greater extent than Dna2 (Figure 2), at least some contribution from an endonucleolytic flap cleavage pathway (i.e. Dna2 or Rad27) is required for cells to progress through S-phase. We reasoned that the requirement for endonucleolytic Okazaki fragment flap processing during S-phase could arise from the accumulation of a small number of long, unprocessed flaps that might persist in *CLB2-RAD27 CLB2-DNA2* cells (20). These long flaps could deplete cellular RPA pools, leading to checkpoint-mediated cell cycle arrest (31) and/or catastrophic failure of replication (32). To test whether excessive exposure of single-stranded DNA was the underlying cause of death in *CLB2-RAD27 CLB2-DNA2* cells, we expressed the *Escherichia coli* single-stranded binding protein SSB from a galactose-inducible promoter. *CLB2-RAD27 CLB2-DNA2 GAL1-SSB* cells were inviable when grown on YPD to repress SSB expression, but viable when SSB was induced by growth on 2% galactose (Figure 4E). Thus, expression of a generic single-strand binding protein restores viability when neither Rad27 nor Dna2 is expressed during early or mid S-phase, indicating that endonucleolytic processing of the lagging strand can be deferred until after the majority of replication has been completed. To test whether this suppression of lethality was solely due to suppression of checkpoint activity, we generated *CLB2-RAD27 CLB2-DNA2 rad9Δ* strains. Un-

like SSB overexpression, deletion of *RAD9* did not restore viability to *CLB2-RAD27 CLB2-DNA2* cells (Figure 4F). This suggests that sequestration of single-stranded DNA, as opposed to checkpoint inactivation, underlies the effect of SSB overexpression on the survival of *CLB2-RAD27 CLB2-DNA2* cells. Because we observed that Okazaki fragment ligation can be similarly deferred (Figure 4A and B), we conclude that both steps of lagging-strand processing can be uncoupled from ongoing DNA replication in *S. cerevisiae*.

DISCUSSION

In this study, we investigated Okazaki fragment processing in the absence of all combinations of the Okazaki fragment nucleases Rad27, Dna2 and Exo1 by carrying out a systematic *in vivo* analysis of Okazaki fragment size, ligatability and terminus location. Similarly to observations *in vitro* (5,19), we observe that strand displacement synthesis by Pol δ is limited by the absence of nucleolytic Okazaki fragment cleavage (Figures 2 and 3). Interestingly, despite a significant reduction in strand-displacement synthesis by Pol δ, Okazaki fragments synthesized in the absence of Rad27 do not have readily ligatable termini (Figure 1B and C). We believe that the most likely scenario is that short flaps persist when both Rad27 and DNA ligase I are absent. However, *RAD27* is not an essential gene in *S. cerevisiae*: therefore,
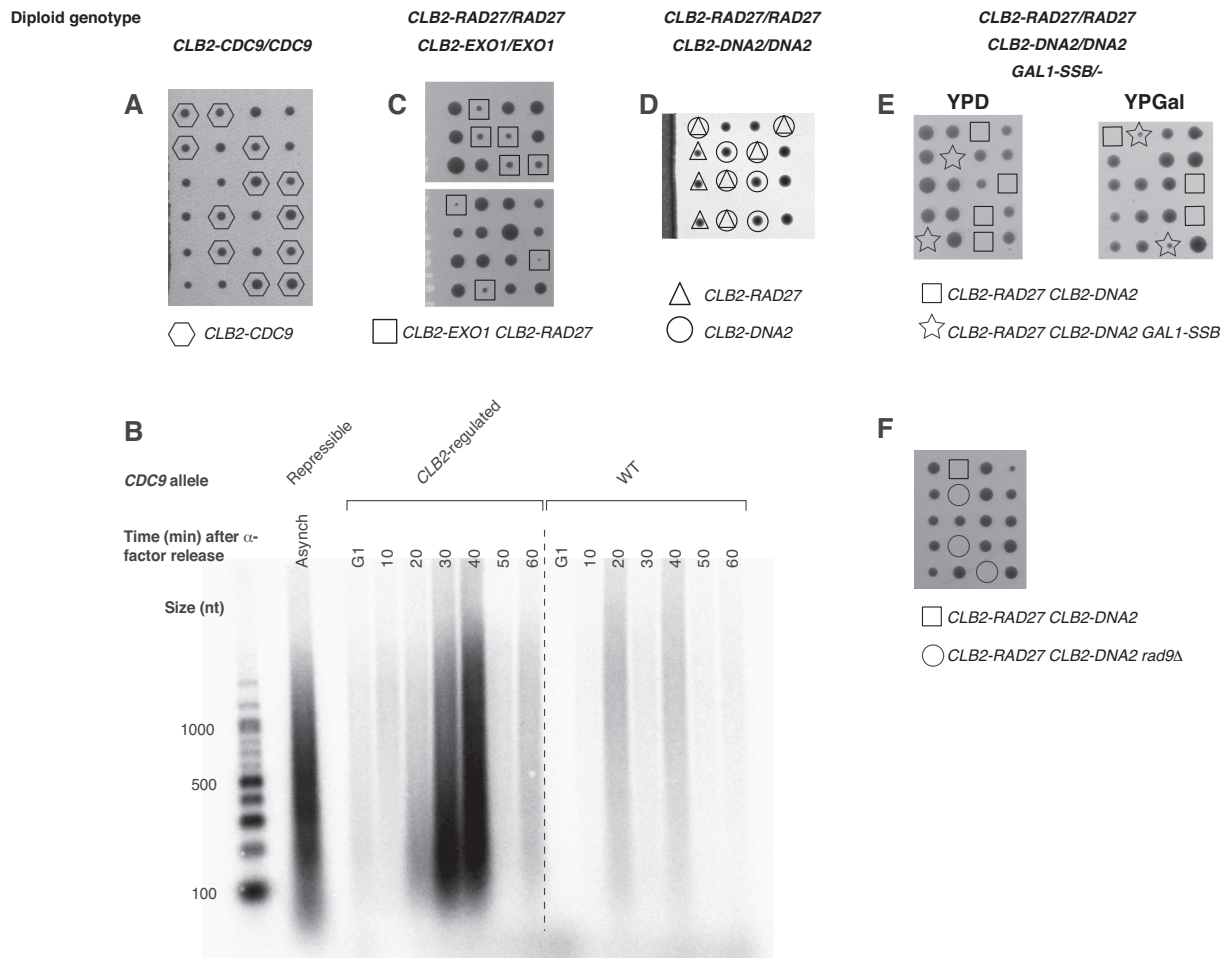
Figure 4. Uncoupling of Okazaki fragment processing and ligation from bulk DNA replication *in vivo*. (**A**) Tetrads from sporulation of a diploid *CLB2-CDC9/CDC9* strain were dissected onto YPD and allowed to grow for 72h. (**B**) *CLB2-CDC9* or wild-type cells were synchronized using alpha-factor, and released into fresh YPD for the indicated time. DNA was purified and end-labeled as in Figure 1B. A sample from an asynchronous culture carrying a doxycycline repressible allele of *CDC9* is shown for comparison. Repression was for 2.5h as previously described (25). (**C, D**) Tetrads from sporulation of a diploid strain heterozygous for (C) *CLB2-RAD27* and *CLB2-EXO1* or (D) *CLB2-RAD27* and *CLB2-DNA2* were dissected onto YPD and allowed to grow for 72h. (**E**) Tetrads from a diploid strain heterozygous for *CLB2-RAD27, CLB2-DNA2* and *GAL1-SSB* were dissected onto either YPD or YPGal plates, as indicated, and allowed to grow for 72h. (**F**) Tetrads from a diploid strain heterozygous for *CLB2-RAD27, CLB2-DNA2* and *rad9δ* were dissected onto YPD and allowed to grow for 72h.

long-lived flaps must eventually be removed in *rad27* cells, presumably by Exo1 or Dna2 in order for *rad27* cells to remain viable.

A strain in which the expression of both flap endonucleases, Rad27 and Dna2, is restricted until after bulk DNA synthesis can only survive when a single-stranded binding protein is overexpressed. Consistent with previous results from *S.pombe* (20), our data suggest that the large majority of Okazaki fragment termini apparently remain closely juxtaposed—either as ligatable nicks or very short flaps—even without significant nuclease processing. However, the inviability of *CLB2-RAD27 CLB2-DNA2* cells and its suppression by SSB overexpression suggests that some long flaps form in the absence of endonucleolytic Okazaki fragment processing, and that the formation of these structures is toxic: we propose that this toxicity stems from RPA depletion as opposed to persistent checkpoint activation, as deletion of *RAD9* does not restore viability to a *CLB2-RAD27 CLB2-DNA2* strain.

Our data suggest that Rad27 and Exo1 have partially redundant activity in Okazaki fragment 5′ flap processing (Figures 2 and 3). If each nuclease acted exclusively on a preferred set of substrates, the most likely outcome would be a bimodal distribution of Okazaki fragment termini in single mutant strains. Substrates normally cleaved by the depleted/deleted nuclease would not be processed, and would show a dramatic change in Okazaki fragment terminus location. Substrates normally cleaved by the other nuclease would be unaffected. We do not observe distributions of Okazaki fragment termini consistent with completely distinct substrates for Rad27 and Exo1. Instead, removal of Exo1 alone has a small but widespread impact on the location of Okazaki fragment termini, while the absence of Rad27 alone shifts a substantial fraction of Okazaki fragment termini towards the replication-fork proximal edge of the nucleosome (Figure 2). Importantly, the most common location of termini in the absence of both nucleases is distinct from that observed in the sole absence of either nu-

cleave (Figure 2). Thus, fragments whose processing is impaired by the absence of Rad27 can apparently still be at least partially processed by Exo1. We propose that distinct Okazaki nucleases do not have rigid substrate preferences, but instead compete to cleave lagging-strand substrates *in vivo*. We note that this model is consistent with the observed suppression of replication-associated *rad27Δ* phenotypes by overexpression of Exo1 (33).

Although Rad27 and Exo1 can redundantly process lagging-strand 5′ flaps, removal of either nuclease leads to a widespread reduction in strand-displacement synthesis by Pol δ, especially in the context of nucleosomes (Figures 2 and 3). The absence of Rad27 reduces strand displacement more than the absence of Exo1. Because each Okazaki fragment is initiated by the error-prone Pol α, such a widespread reduction in nick translation by Pol δ would most likely increase the extent to which DNA synthesized by Pol α is transmitted to daughter cells. Both *rad27Δ* (26) and *exo1Δ* (33) strains are mutators, and the phenotype of *rad27Δ* is notably more severe than that of *exo1Δ*. Given the correlation between the strength of the mutator phenotype and the extent to which strand-displacement by Pol δ is reduced, we speculate that retention of genomic DNA synthesized by Pol α underlies the elevated mutation rates observed when these genes are absent. Consistent with this model, temperature-sensitive *dna2* strains are not mutators (17) and depletion of Dna2 does not significantly alter global strand displacement *in vivo* (Figures 2 and 3).

We observe that the contribution of Dna2 to Okazaki fragment processing is extremely limited in the uniquely mappable regions of the genome that can be assayed using our sequencing methodology (Figures 2 and 3). In addition, *CLB2-DNA2* cells do not have a detectable growth defect (Figure 4D). Therefore, although the nuclease activity of Dna2 is essential for viability in checkpoint-proficient cells (34), the absence of Dna2 during S-phase is not obviously detrimental to exponentially dividing *S. cerevisiae* cells. It is possible that Dna2 is required for the cleavage of only a small number of Okazaki fragment 5′ flaps – either long flaps generated by low levels of ongoing strand displacement without nuclease cleavage, or those in specific, late-replicating repeat regions such as telomeres (35,36) or the rDNA repeat (37).

DATA AVAILABILITY

Sequencing data are available from GEO under accession number GSE118078.

SUPPLEMENTARY DATA

Supplementary Data are available at NAR Online.

ACKNOWLEDGEMENTS

FUNDING

REFERENCES

1. Burgers,P.M. (2009) Polymerase dynamics at the eukaryotic DNA replication fork. *J. Biol. Chem.*, **284**, 4041–4045.
2. Nethanel,T. and Kaufmann,G. (1990) Two DNA polymerases may be required for synthesis of the lagging DNA strand of simian virus 40. *J. Virol.*, **64**, 5912–5918.
3. Singh,H., Brooke,R.G., Pausch,M.H., Williams,G.T., Trainor,C. and Dumas,L.B. (1986) Yeast DNA primase and DNA polymerase activities. An analysis of RNA priming and its coupling to DNA synthesis. *J. Biol. Chem.*, **261**, 8564–8569.
4. Maga,G., Stucki,M., Spadari,S. and Hubscher,U. (2000) DNA polymerase switching. I. Replication factor C displaces DNA polymerase alpha prior to PCNA loading. *J. Mol. Biol.*, **295**, 791–801.
5. Garg,P., Stith,C.M., Sabouri,N., Johansson,E. and Burgers,P.M. (2004) Idling by DNA polymerase delta maintains a ligatable nick during lagging-strand DNA replication. *Genes Dev.*, **18**, 2764–2773.
6. Kao,H.I., Veeraraghavan,J., Polaczek,P., Campbell,J.L. and Bambara,R.A. (2004) On the roles of Saccharomyces cerevisiae Dna2p and Flap endonuclease 1 in Okazaki fragment processing. *J. Biol. Chem.*, **279**, 15014–15024.
7. Johnston,L.H. and Nasmyth,K.A. (1978) Saccharomyces cerevisiae cell cycle mutant cdc9 is defective in DNA ligase. *Nature*, **274**, 891–893.
8. Balakrishnan,L., Stewart,J., Polaczek,P., Campbell,J.L. and Bambara,R.A. (2010) Acetylation of Dna2 endonuclease/helicase and flap endonuclease 1 by p300 promotes DNA stability by creating long flap intermediates. *J. Biol. Chem.*, **285**, 4398–4404.
9. Bae,S.H., Bae,K.H., Kim,J.A. and Seo,Y.S. (2001) RPA governs endonuclease switching during processing of Okazaki fragments in eukaryotes. *Nature*, **412**, 456–461.
10. Rossi,M.L. and Bambara,R.A. (2006) Reconstituted Okazaki fragment processing indicates two pathways of primer removal. *J. Biol. Chem.*, **281**, 26051–26061.
11. Ayyagari,R., Gomes,X.V., Gordenin,D.A. and Burgers,P.M. (2003) Okazaki fragment maturation in yeast. I. Distribution of functions between FEN1 AND DNA2. *J. Biol. Chem.*, **278**, 1618–1625.
12. Gloor,J.W., Balakrishnan,L., Campbell,J.L. and Bambara,R.A. (2012) Biochemical analyses indicate that binding and cleavage specificities define the ordered processing of human Okazaki fragments by Dna2 and FEN1. *Nucleic Acids Res.*, **40**, 6774–6786.
13. Levikova,M. and Cejka,P. (2015) The Saccharomyces cerevisiae Dna2 can function as a sole nuclease in the processing of Okazaki fragments in DNA replication. *Nucleic Acids Res.*, **43**, 7888–7897.
14. Budd,M.E., Antoshechkin,I.A., Reis,C., Wold,B.J. and Campbell,J.L. (2011) Inviability of a DNA2 deletion mutant is due to the DNA damage checkpoint. *Cell Cycle*, **10**, 1690–1698.
15. Formosa,T. and Nittis,T. (1999) Dna2 mutants reveal interactions with Dna polymerase alpha and Ctf4, a Pol alpha accessory factor, and show that full Dna2 helicase activity is not essential for growth. *Genetics*, **151**, 1459–1470.
16. Budd,M.E. and Campbell,J.L. (2000) The pattern of sensitivity of yeast dna2 mutants to DNA damaging agents suggests a role in DSB and postreplication repair pathways. *Mutat. Res.*, **459**, 173–186.
17. Budd,M.E., Tong,A.H., Polaczek,P., Peng,X., Boone,C. and Campbell,J.L. (2005) A network of multi-tasking proteins at the DNA replication fork preserves genome stability. *PLoS Genet.*, **1**, e61.
18. Parenteau,J. and Wellinger,R.J. (1999) Accumulation of single-stranded DNA and destabilization of telomeric repeats in yeast mutant strains carrying a deletion of RAD27. *Mol. Cell. Biol.*, **19**, 4143–4152.
19. Stodola,J.L. and Burgers,P.M. (2016) Resolving individual steps of Okazaki-fragment maturation at a millisecond timescale. *Nat. Struct. Mol. Biol.*, **23**, 402–408.
20. Liu,B., Hu,J., Wang,J. and Kong,D. (2017) Direct visualization of RNA-DNA primer removal from okazaki fragments provides

support for flap cleavage and exonucleolytic pathways in eukaryotic cells. *J. Biol. Chem.*, **292**, 4777–4788.

21. Callegari,A.J., Clark,E., Pneuman,A. and Kelly,T.J. (2010) Postreplication gaps at UV lesions are signals for checkpoint activation. *Proc. Natl. Acad. Sci. U.S.A.*, **107**, 8219–8224.

22. Lopes,M., Foiani,M. and Sogo,J.M. (2006) Multiple mechanisms control chromosome integrity after replication fork uncoupling and restart at irreparable UV lesions. *Mol. Cell*, **21**, 15–27.

23. Taylor,M.R.G. and Yeeles,J.T.P. (2018) The initial response of a eukaryotic replisome to DNA damage. *Mol. Cell*, **70**, 1067–1080.

24. Daigaku,Y., Davies,A.A. and Ulrich,H.D. (2010) Ubiquitin-dependent DNA damage bypass is separable from genome replication. *Nature*, **465**, 951–955.

25. Smith,D.J. and Whitehouse,I. (2012) Intrinsic coupling of lagging-strand synthesis to chromatin assembly. *Nature*, **483**, 434–438.

26. Reagan,M.S., Pittenger,C., Siede,W. and Friedberg,E.C. (1995) Characterization of a mutant strain to Saccharomyces Cerevisiae with a deletion of the RAD27 gene, a structural homolog of the RAD2 nucleotide excision-repair gene. *J. Bacteriol.*, **177**, 364–371.

27. Haruki,H., Nishikawa,J. and Laemmli,U.K. (2008) The anchor-away technique: rapid, conditional establishment of yeast mutant phenotypes. *Mol. Cell*, **31**, 925–932.

28. Osmundson,J.S., Kumar,J., Yeung,R. and Smith,D.J. (2017) Pif1-family helicases cooperatively suppress widespread replication-fork arrest at tRNA genes. *Nat. Struct. Mol. Biol.*, **24**, 162–170.

29. Karras,G.I. and Jentsch,S. (2010) The RAD6 DNA damage tolerance pathway operates uncoupled from the replication fork and is functional beyond S phase. *Cell*, **141**, 255–267.

30. Willer,M., Rainey,M., Pullen,T. and Stirling,C.J. (1999) The yeast CDC9 gene encodes both a nuclear and a mitochondrial form of DNA ligase I. *Curr. Biol.*, **9**, 1085–1094.

31. Byun,T.S., Pacek,M., Yee,M.C., Walter,J.C. and Cimprich,K.A. (2005) Functional uncoupling of MCM helicase and DNA polymerase activities activates the ATR-dependent checkpoint. *Genes Dev.*, **19**, 1040–1052.

32. Toledo,L., Altmeyer,M., Rask,M.-B., Lukas,C., Larsen,D., Povlsen,L., Bekker-Jensen,S., Mailand,N., Bartek,J. and Lukas,J. (2013) ATR prohibits replication catastrophe by preventing global exhaustion of RPA. *Cell*, **155**, 1088–1103.

33. Tishkoff,D.X., Boerger,A.L., Bertrand,P., Filosi,N., Gaida,G.M., Kane,M.F. and Kolodner,R.D. (1997) Identification and characterization of Saccharomyces cerevisiae EXO1, a gene encoding an exonuclease that interacts with MSH2. *Proc. Natl. Acad. Sci. U.S.A.*, **94**, 7487–7492.

34. Budd,M.E., Choe,W. and Campbell,J.L. (2000) The nuclease activity of the yeast DNA2 protein, which is related to the RecB-like nucleases, is essential in vivo. *J. Biol. Chem.*, **275**, 16518–16529.

35. Budd,M.E. and Campbell,J.L. (2013) Dna2 is involved in CA strand resection and nascent lagging strand completion at native yeast telomeres. *J. Biol. Chem.*, **288**, 29414–29429.

36. Markiewicz-Potoczny,M., Lisby,M. and Lydall,D. (2018) A critical role for Dna2 at unwound telomeres. *Genetics*, **209**, 129–141.

37. Villa,F., Simon,A.C., Ortiz Bazan,M.A., Kilkenny,M.L., Wirthensohn,D., Wightman,M., Matak-Vinković,D., Pellegrini,L. and Labib,K. (2016) Ctf4 is a hub in the eukaryotic replisome that links multiple CIP-Box proteins to the CMG helicase. *Mol. Cell*, **63**, 385–396.

38. Jiang,C. and Pugh,B.F. (2009) A compiled and systematic reference map of nucleosome positions across the Saccharomyces cerevisiae genome. *Genome Biol.*, **10**, R109.

39. MacIsaac,K.D., Wang,T., Gordon,D.B., Gifford,D.K., Stormo,G.D. and Fraenkel,E. (2006) An improved map of conserved regulatory sites for Saccharomyces cerevisiae. *BMC Bioinformatics*, **7**, 113.